Exceptional ancient DNA preservation and fibre remains of a Sasanian saltmine sheep mummy in Chehrābād, Iran

Conor Rossi[1], Gabriela Ruß-Popa[2], Valeria Mattiangeli[1], Fionnuala McDaid[1], Andrew J. Hare[1], Hossein Davoudi[3], Haeedeh Laleh[3,4], Zahra Lorzadeh[3], Roya Khazaeli[3], Homa Fathi[3], Matthew D. Teasdale[5], Abolfazl A'ali[6], Thomas Stöllner[7], Marjan Mashkour[3,8], Kevin G. Daly[1]

1. Smurfit Institute of Genetics, Trinity College Dublin, Dublin 2, Ireland
2. Austrian Academy of Sciences, Austrian Archaeological Institute, Archaeological Sciences, Hollandstraße 11-13, 1020 Vienna, Austria
3. University of Tehran, Central Laboratory, Bioarchaeology Laboratory, 1417634934 Tehran, Iran
4. University of Tehran, Faculty of Humanities, Department of Archaeology, 1417935840 Tehran, Iran
5. McDonald Institute for Archaeological Research, Dept. of Archaeology, University of Cambridge
6. Zanjan Cultural Heritage Centre, Archaeological Museum of Zanjan, Emaarate Zolfaghari,Taleghani St., Zanjan, Iran
7. Ruhr University Bochum, Institute for Archaeological Studies & Deutsches Bergbau-Museum Bochum, Research Department, Haus der Archäologien, Am Bergbaumuseum 31, D-44791 Bochum
8. Archéozoologie, Archéobotanique, Sociétés, Pratiques et Environnements (AASPE), Muséum national d'Histoire naturelle, Sorbonne Université, CNRS; CP 56, 55 rue Buffon, 75005 Paris, France

Abstract

Mummified remains have long attracted interest as a potential source of ancient DNA. However, mummification is a rare process that requires an anhydrous environment to rapidly dehydrate and preserve tissue before complete decomposition occurs. We present the whole genome sequences of a ~1600 year old naturally mummified sheep recovered from Chehrābād, a salt mine in northwestern Iran. Comparative analyses of published ancient sequences revealed remarkable DNA integrity of this mummy. Hallmarks of postmortem damage, fragmentation and hydrolytic deamination, are substantially reduced, likely due to the high-salinity of this taphonomic environment. Metagenomic analyses reflect the profound influence of high salt content on decomposition; its microbial profile is predominated by halophilic archaea and bacteria, possibly contributing to the remarkable preservation of this sample. Applying population genomic analyses we find consistent clustering of this sheep with Southwest Asian modern breeds, suggesting ancestry continuity. Genotyping of a locus influencing the woolly phenotype showed the existence of an ancestral "hairy" allele in this sheep, consistent with hair fibre imaging, further elucidating Sasanian-period animal husbandry.

Introduction

In 1993, a remarkably preserved human body dating to the ~1700 years Before Present (BP) was discovered in the Douzlākh salt mine near Chehrābād village in the Zanjan Province of northwest Iran [1–3]. A total of 8 "Salt Men" have been identified at the mine [4,5], several retaining keratinous tissues such as skin, hair, and both endo- and exoparasites, despite dating to the Achaemenid (550-330 BCE, 2500-2280 BP) and Sasanian (224-651 CE, ~1700-1300 BP) periods. The mine, also known as Chehrābād, was active in various periods and its archaeological refilling layers represent an extraction history that ranged from the 6th century BCE to 20th century CE. In addition to the "Salt Men", textiles, leather objects, and animal remains have been discovered [6,7], likely preserved by high salinity and low moisture content of the mine. Isotopic, genetic, and lipid analyses have been reported for this material [1], and studies have been carried out to characterize genomic DNA survival [8]. These human and animal remains are examples of natural mummification - the spontaneous desiccation of soft tissue by a dry environment that rapidly dehydrates soft tissue before decay begins [9].

Mummification has been suggested as a mechanism that may sufficiently preserve keratinised tissue for ancient DNA (aDNA) sequencing [9]. The effects of age-related damage in aDNA are well documented and include base misincorporation at strand overhangs, fragmentation and low endogenous content [10]. Both deamination and depurination, associated with postmortem transition error and DNA fragmentation, respectively, require water as a substrate [11]. Ancient DNA from Chehrābād, a highly saline, anhydrous environment, presents an opportunity to investigate potential differences in nucleotide degradation resulting from this unusual taphonomic context.

In this study we sequenced DNA from the ~1600 year old (Sasanian period) mummified sheep leg 4305, recently discovered in a large mining gallery in the northwestern edge of the Douzlākh saltmine of Chehrābād by Iranian-German researchers during archaeological excavations (Fig. 1A) [2]. The specimen was likely deposited during refilling activities in the 4-5th centuries CE after the gallery's reopening in the Early Sasanian period (2nd-3rd centuries CE) and following its initial collapse between 405-380 BCE. The leg was possibly discarded during food preparation activities, as both sheep and goat were likely used as provisioning for Sasanian-period miners; equines may have been used as beasts of burden [12]. We find unusual survival patterns of endogenous DNA given its distance from the equator, implying exceptional preservation of nucleic acid integrity was afforded by the unique salt-rich environment. This enables population genomic profiling of this sheep including genotyping the antisense *EIF2S2* retrogene insertion within the 3' UTR of the *IRF2BP2* gene which influences the woolly phenotype [13], in tandem with fibre analysis using scanning electron microscopy (SEM), and characterising the mummy skin metagenome.

Materials & Methods

A sample of the mummified sheep skin (Table 1, MUM2) from sheep leg 4305 was directly radiocarbon dated at the ^{14}CHRONO Centre (Queen's University Belfast). OxCal 4.3.2 [14] was used to calibrate its age (95.4% confidence interval) using [15].

Sample preparation, extraction and library preparation were performed in a dedicated aDNA laboratory in the Smurfit Institute of Genetics, Trinity College Dublin according

to standard protocols (supplementary material). Sequencing of MUM2 and two Iranian sheep bone samples (Khor1 and Azer2) of approximately similar age (Table 1) for comparison was performed on Illumina MiSeq (50bp SE) and HiSeq 2500 platforms (100bp SE and 100bp PE).

Sequencing reads were aligned to OviAri3.1 and filtered to produce bam files following standard aDNA sequencing pipelines (supplementary material). Damage patterns were assessed using mapDamage2.0 [16].

Filtered reads not aligned to either sheep or human genomes were taxonomically assigned using the metagenomic classifier Kraken2 [17]. Microbial sources were estimated using SourceTracker2 [18] with a custom metagenomic database [19] [20] [21] [22] [23] (supplementary material). Bacterial species abundances were generated using MIDAS [24].

Mitochondrial sequences were produced using ANGSD [25] and a Maximum-Likelihood phylogenetic tree was generated using SeaView and phyML [26–28] with the HKY85 substitution model, selected using jmodeltest2 [29,30] and 100 bootstrap repeats.

A SNP dataset of modern breeds [31] was used to investigate genomic affinities (supplementary material). LASER (v2.03) PCA [32], outgroup f_3 statistics [33], TreeMix [34] and ADMIXTURE [35] analyses were completed (supplementary material).

We investigated the woolly locus located on chromosome 25 [13]. Two modified OviAri3.1 assemblies were produced, one representing the ancestral “hairy” phenotype, the other representing the “woolly” phenotype (supplementary material). Final bam files were visualised using IGV [36]. Hair fibres were examined using scanning electron and light microscopes at USTEM, TU Wien and Austrian Archaeological Institute respectively.

Results and Discussion

The Chehrābād mummy sample (MUM2) was directly dated to the 5-6th century CE (2 sigma 1621-1481 cal BP, uncalibrated 1600 ± 30 BP, Supplementary Figure 3). This aligns with the Sasanian Empire period of Iran, a time when the mine was in active use [1]. Initial DNA screening indicated high endogenous DNA for MUM2, and also the comparative Iranian sheep samples from relatively close time periods (Table 1).

Name	Tissue	Origin	Period	Age	Endogenous DNA %	Coverage (X)
MUM2	Mummified skin	Chehrābād, Iran	Sasanian Empire period	*399-539 cal CE	31.01	3.94
Khor1	Petrous bone	Nishapur, Iran	Sasanian - Islamic periods	600 - 1200 CE	58.44	0.04
Azer2	Petrous bone	Tepe Hasanlu, Iran	Iron Age III	800-600 BCE	31.32	0.07

Table 1. Summary information of samples sequenced in this study. * = directly dated.

Sequencing of the Chehrābād mummy produced a 3.94X genome after quality filtering (Supplementary Table 1), in addition to the low coverage comparative genomes (0.04X and 0.07X). MUM2 differs from the two comparative sheep samples in displaying longer fragment lengths (median 107bp vs 52bp and 56bp; Figure 1B; collapsed reads-only 90bp vs 50bp and 55bp) and substantially lower rates of deamination (Figure 1D) (δS, single strand cytosine deamination probability, mean δS = 0.012 vs. 0.382 and 0.334). Contrasting previously published ancient ovicaprid data from Southwest Asia and Europe (Supplementary Table 3), MUM2 falls outside the ranges of both median fragment length and mean δS values (Figure 1C and 1E), indicating remarkably low fragmentation and deamination of the Chehrābād sheep mummy genomic material given its latitude. Similar length distributions have been reported primarily from high latitude and permafrost environments [37–40]. A low level of thermal fluctuations may also contribute to DNA preservation [41], as comparable fragment lengths have been reported in a human sample from Wezmeh Cave, Iran [42].

Recent models of postmortem DNA fragmentation suggest rate-constant hydrolytic depurination over time [43], or age-independent, driven by environment-dependent biotic and abiotic factors [41]. The depurination rates of MUM2 are similar to the more-fragmented comparative samples (Supplementary Figure 4), implying that other processes in the Chehrābād environment underlie the lower fragmentation rates. The highly alkaline, cool and anhydrous conditions may have contributed to inhibition of cellular nucleases which would otherwise degrade and fragment endogenous DNA [9]. Postmortem DNA deamination via cytosine hydrolysis [44] is thought to be strongly correlated with age [45] and thermal age [41]. The substantially-lower rates of deamination observed in MUM2 is likely due to the scarcity of environmental free water, required for hydrolytic deamination. These results are consistent with Chehrābād providing a taphonomic environment conducive to genome preservation.

DNA preservation may also be influenced by its tissue-of-origin; for example, bone hydroxyapatite rather than keratin fractions are associated with smaller fragment size [46]. As hydrophobic keratinised tissue may provide resistance to environmental water [47], we compared MUM2 to published ancient skins genomes (Figure 1F) to determine if tissue providence was solely responsible for DNA preservation. The mean δS of MUM2 falls outside the range of other ancient skin genomes, including 20th century CE goat skins [48] and leather recovered from the Tyrolean Iceman [49]. While this does not discount keratinized tissue being specifically enriched with longer DNA fragments, the Chehrābād sheep mummy appears to be singular in its DNA integrity among published skin samples.

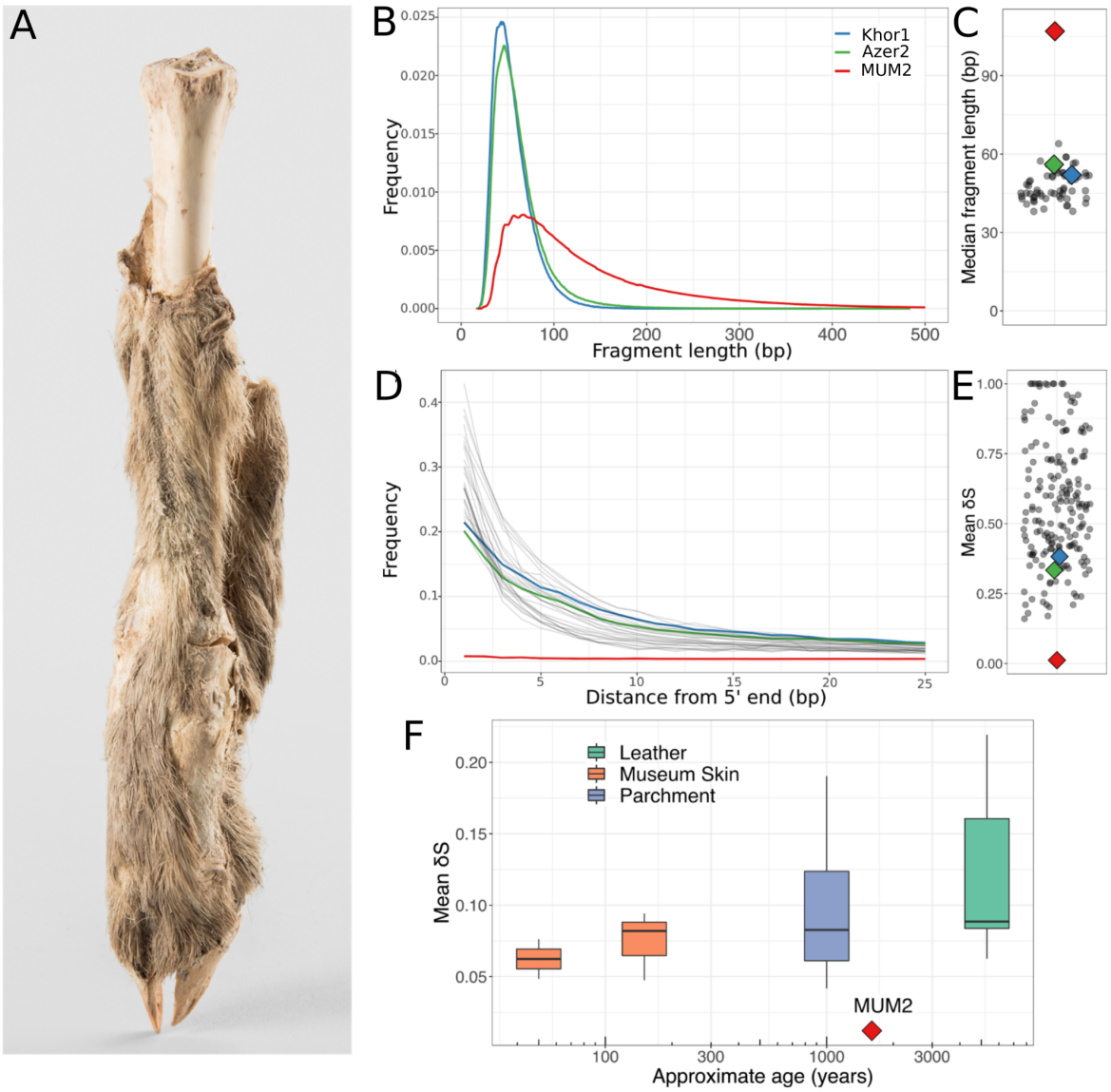

Figure 1 (A) Mummified sheep leg (4305) after cleaning. Photography: N. Tehrani **(B) Read length distributions of MUM2, Khor1, and Azer2, calculated from PE data.** MUM2 shows a reduced rate of fragmentation. The median read length of MUM2 (107 bp) exceeds the median read length of Khor1 and Azer2 (52 bp & 56 bp, respectively). **(C) Median read lengths of 61 published ancient Ovicaprid samples** [50]**.** The median read length of MUM2 (107 bp; 90 bp among collapsed reads only) exceeds the longest among published ovicaprid genomes (64 bp). **(D) Deamination patterns of MUM2, Khor1, Azer2, and other ancient ovicaprids for non UDG-treated libraries.** Low levels of base misincorporation at the 5' ends of reads were observed for MUM2 compared to Khor1 and Azer2. **(E) Mean δS of published 182 ancient bone samples** [50] [41]**.** The mean δS of MUM2 (0.012) is singular in its low levels of deamination. **(F) Comparison of mean δS of published ancient skins** [51] [49] [48]. Lower damage rates are recorded compared to all samples, including some ~50 years old.

Given the distinctive geochemical composition of Chehrābād, we examined if its salt-rich environment was reflected in the metagenomic profile of MUM2. Taxonomic assignment and abundance estimation assigned 57.13% of classified reads to the halophilic Class of Archaea *Halobacteria* (Supplementary Table 2). Similarly, SourceTracker2 predicted that 0.4725 - 0.7458 of the microbial community originated from a salt-rich environment (Table 2, Supplementary Figure 5). A complementary analysis using MIDAS identified 76 unique bacterial species in the mummified sheep (Supplementary Table 4). The most abundant species is the halophilic bacterium *Actinopolyspora halophila 58532,* accounting for ~29% of identified reads. This signal of a dominant halophilic microbial community is not replicated in comparison samples or controls (Table 2, supplementary material). Rapid colonization by saprophytic microbial communities, with key decomposers being ubiquitous across soil types, is typical for mammalian corpses post-mortem [52]. The halophilic metagenome profile observed in the Chehrābād sheep mummy skin indicates that the typical decomposers may be less abundant in this alkaline, salt-rich setting, which may have contributed to soft tissue and molecular preservation.

	MUM2 (Species)	**Azer2 (Species)**	**Khor1 (Species)**	**MUM2 (Genus)**	**Azer2 (Genus)**	**Khor1 (Genus)**
Tissue decomposers	0.0212	0.1458	0.0386	0.0426	0.3524	0.3727
Salt-rich	0.4725	0.0026	0.0036	0.7458	0.0145	0.0151
Laboratory reagents	0.0003	0.0002	0.0002	N/A	N/A	N/A
Sheep skin	0.0285	0.085	0.0463	0.0829	0.3294	0.2244
Soil	0.0009	0.0007	0.0046	0	0	0
Unknown	0.4766	0.7657	0.9067	0.1287	0.3037	0.3878

Table 2: Predicted source proportion of metagenomic reads by SourceTracker2.

Population genomics

We investigated how the Chehrābād sheep MUM2 relates to modern populations using mitochondrial and autosomal variation. A 664X mitochondrial genome of MUM2 falls within the C haplotype cluster in a Maximum-Likelihood phylogeny of

modern sheep mitochondria (Supplementary Figure 7). This clade is found at its highest frequency in southwest and east Asia [53,54], and has been reported in ancient samples from Bronze Age Turkey [55], and is consistent with past and present-day patterns of mitochondrial diversity.

PCA from autosomal variation clusters MUM2 with modern southwest Asian breeds, using both global and Asian reference panels (Supplementary Figure 8). f_3 outgroup statistics show MUM2 shares the most genetic drift with southwest Asian breeds, particularly those from Iran (Figure 2A). ADMIXTURE and TreeMix analysis also confirmed the affinity of MUM2 with modern sheep breeds from southwest Asia, particularly the Qezel and Afec-Assaf breeds sampled from Iran [31] (supplementary material). Overall, there is genetic continuity between west Iranian sheep populations in Sassanid and modern time periods, although PCA using Ovine SNP50 genotypes of Asian breeds place MUM2 apart from sampled breeds (Supplementary Figure 9), suggesting a degree of genetic flux during the past 1500-1600 years in Iranian sheep.

Fibre Genotype and Phenotype

The derived "woolly" coat phenotype is thought to be influenced by a ~1.5 kbp insertion of a *EIF2S2* retrogene into the *IRF2BP2* 3' UTR, recessive to the ancestral allele associated with "hairy" coat [13]. We exploited the length of the MUM2 DNA fragments to investigate this "woolly" locus by searching for read pairs which either encompassed or overlapped the insertion breakpoint, indicative of a copy of the "hairy" allele. No reads were found to overlap the diagnostic insertion breakpoints of the "woolly" insert, which would indicate a copy of the "woolly" allele (Figure 2B). Five reads were found to uniquely map to the 'hairy' allele diagnostic position, with a further two read pairs inferred to overlap this breakpoint (Figure 2C). We therefore infer this animal to be either homozygous or heterozygous for the dominant "hairy" allele. In addition, SEM imaging of the mostly-unpigmented mummified hair fibres revealed mosaic scales typical of sheep [56] with fine lines on the scale surface (Figure 2D, supplementary material), a characteristic of sheep hair fibres and particularly for mouflon and medium-wool breeds [57]. This may reflect MUM2 coming from a herd maintained for meat or milk production rather than wool,

consistent with suggestions that ovicaprids were used as food for workers, and that sections of the mine were used as stables [1].

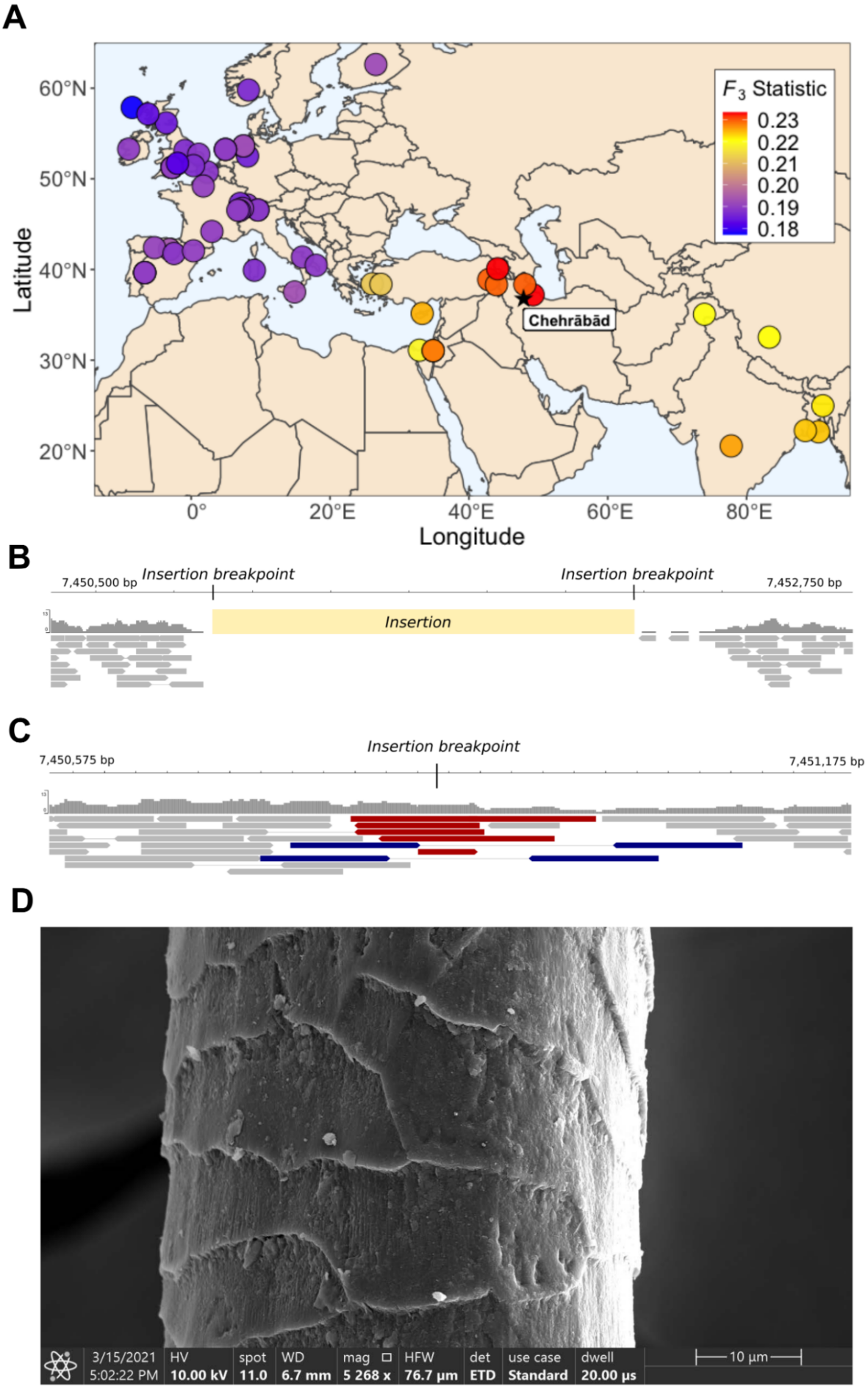
A
60°N
50°N
40°N
30°N
20°N
Latitude
0°
20°E
40°E
60°E
80°E
Longitude
F_3 Statistic
0.23
0.22
0.21
0.20
0.19
0.18
Chehrābād
B
7,450,500 bp
Insertion breakpoint
Insertion breakpoint
7,452,750 bp
Insertion
C
7,450,575 bp
Insertion breakpoint
7,451,175 bp
D
3/15/2021 5:02:22 PM
HV 10.00 kV
spot 11.0
WD 6.7 mm
mag 5 268 x
HFW 76.7 µm
det ETD
use case Standard
dwell 20.00 µs
10 µm

Figure 2. (A) Shared genetic drift between MUM2 and modern sheep populations. Higher f_3 values, in red, indicate higher shared drift, relative to the outgroup Asiatic Mouflon. **Visualisation of read coverage of filtered bam files at woolly locus, in assemblies with (B) and without (C) the insertion.** Reads highlighted in red overlap the insertion breakpoint, blue indicates an inferred overlap of the insertion point by the straddling read pair. Highlighted reads map only to one assembly and do not align to the other. (**D) SEM image of MUM2 hair fibre, displaying the mosaic scales typical of a sheep hair shaft.** Image by A. Steiger-Thirsfeld and G. Ruß-Popa.

The Chehrābād saltmine provides a remarkable case study of the importance of taphonomic context for tissue and genetic preservation. We exploit this to investigate both the hair fibre genotype and phenotype of this natural sheep mummy, thus intimating at its likely use as a food source for Sassian-period miners.

Data Accessibility: Sequencing reads and mitochondrial sequences are available under European Nucleotide Archive accession PRJEB43881. MDT was additionally supported by ERC investigator grant no. 787282-B2C.

Funding: Supported by ERC Investigator grant 295729-CodeX.

Authors' contribution: CR, KGD, and MM designed study; CR, KGD, VM, AH, and FM performed laboratory work; CR and MDT performed bioinformatic work; GRP was responsible for SEM analysis; HD, HL, ZL, RK, HF, AA, TS, and MM worked directly with and provided archaeological samples. All authors contributed to writing the manuscript, approve this study, and are accountable for all aspects of the work.

Acknowledgements: We thank Andreas Steiger-Thirsfeld for SEM images and N. Tehrani for sample photography.

References

1. Aali A, Stöllner T, Abar A, Rühli F. 2012 The Salt Men of Iran: The Salt Mine of Douzlākh, Chehrābād. **42**, 61–81.

2. Aali A, Stöllner T. 2015 *The Archaeology of the Salt Miners: Interdisciplinary Research 2010-2014*. Bochum: Deutsches Bergbau-Museum.

3. Stöllner T, Aali A, Bagherpour Kashani N. 2020 *Tod im Salz. Eine archäologische Ermittlung in Persien. Begleitbuch, Katalog und Graphic Novel*. Bochum: Nünnerich-Asmus Verlag Media.

4. Öhrström LM, Seiler R, Böni T, Aali A, Stöllner T, Rühli FJ. 2016 Erratum to: Radiological findings in an ancient Iranian salt mummy (Chehrābād ca. 410-350 BC). *Skeletal Radiol.* **45**, 433.

5. Nasab HV, Aali A, Kazzazi M, Pollard M, Stöllner T. 2019 Reappraisal of the number of salt mummies identified in Chehrābād Salt Mine, Zanjan, Iran. *Bioarchaeology of the Near East* **13**, 23–47.

6. Mashkour M. 2014 Faunal report of the 2010 and 2011 excavation campaigns. In *The Archaoelogy of the salt miners* (eds A Aali, T Stöllner), pp. 112–117. Bochum: Metatta.

7. Mashkour M, Fathi H, Davoudi H. 2020 Interaktionen zwischen Mensch und Tier im Salzbergwerk Douzlākh, Chehrābād. In *Tod im Salz. Eine archäologische Ermittlung in Persien. Begleitbuch, Katalog und Graphic Novel* (ed Stöllner T, Aali A, Bagherpour Kashani N), pp. 219–224.

8. Warinner C, Bouwman A. 2015 Ancient DNA Investigation of the Chehrābād Mummies: Interim Report. In *The Archaeology of the Salt Miners: Interdisciplinary Research 2010-2014* (eds A Aali, T Stöllner), pp. 90–96. Bochum: Deutsches Bergbau-Museum.

9. David R. 2008 *Egyptian Mummies and Modern Science*. Cambridge University Press.

10. Dabney J, Meyer M, Pääbo S. 2013 Ancient DNA damage. *Cold Spring Harb. Perspect. Biol.* **5**. (doi:10.1101/cshperspect.a012567)

11. Dabney J, Meyer M, Pääbo S. 2013 Ancient DNA damage. *Cold Spring Harb. Perspect. Biol.* **5**. (doi:10.1101/cshperspect.a012567)

12. Nezamabadi M, Aali A, Stöllner T, Mashkour M, Le Bailly M. 2013 Paleoparasitological analysis of samples from the Chehrabad salt mine (Northwestern Iran). *Int J Paleopathol* **3**, 229–233.

13. Demars J *et al.* 2017 Genome-Wide Identification of the Mutation Underlying Fleece Variation and Discriminating Ancestral Hairy Species from Modern Woolly Sheep. *Mol. Biol. Evol.* **34**, 1722–1729.

14. Ramsey CB. 2009 Bayesian Analysis of Radiocarbon Dates. *Radiocarbon*. **51**, 337–360. (doi:10.1017/s0033822200033865)

15. Reimer PJ *et al.* 2013 IntCal13 and Marine13 Radiocarbon Age Calibration Curves 0–50,000 Years cal BP. *Radiocarbon* **55**, 1869–1887.

16. Jónsson H, Ginolhac A, Schubert M, Johnson PLF, Orlando L. 2013 mapDamage2.0: fast approximate Bayesian estimates of ancient DNA damage parameters. *Bioinformatics* **29**, 1682–1684.

17. Wood DE, Lu J, Langmead B. 2019 Improved metagenomic analysis with Kraken 2. *Genome Biol.* **20**, 257.

18. Knights D, Kuczynski J, Charlson ES, Zaneveld J, Mozer MC, Collman RG, Bushman FD, Knight R, Kelley ST. 2011 Bayesian community-wide culture-independent microbial source tracking. *Nat. Methods* **8**, 761–763.

19. Emmons AL, Mundorff AZ, Keenan SW, Davoren J, Andronowski J, Carter DO, DeBruyn JM. 2020 Characterizing the postmortem human bone microbiome from surface-decomposed remains. *PLoS One* **15**, e0218636.

20. Robinson CK *et al.* 2015 Microbial diversity and the presence of algae in halite endolithic communities are correlated to atmospheric moisture in the hyper-arid zone of the Atacama Desert. *Environ. Microbiol.* **17**, 299–315.

21. Ross AA, Müller KM, Scott Weese J, Neufeld JD. 2018 Comprehensive skin microbiome analysis reveals the uniqueness of human skin and evidence for phylosymbiosis within the class Mammalia. *Proc. Natl. Acad. Sci. U. S. A.* **115**, E5786–E5795.

22. Moreira-Grez B, Tam K, Cross AT, Yong JWH, Kumaresan D, Nevill P, Farrell M, Whiteley AS. 2019 The Bacterial Microbiome Associated With Arid Biocrusts and the Biogeochemical Influence of Biocrusts Upon the Underlying Soil. *Front. Microbiol.* **10**. (doi:10.3389/fmicb.2019.02143)

23. Salter SJ *et al.* 2014 Reagent and laboratory contamination can critically impact sequence-based microbiome analyses. *BMC Biol.* **12**, 1–12.

24. Nayfach S, Rodriguez-Mueller B, Garud N, Pollard KS. 2016 An integrated metagenomics pipeline for strain profiling reveals novel patterns of bacterial transmission and biogeography. *Genome Res.* **26**, 1612–1625.

25. Korneliussen TS, Albrechtsen A, Nielsen R. 2014 ANGSD: Analysis of Next Generation Sequencing Data. *BMC Bioinformatics* **15**, 356.

26. Edgar RC. 2004 MUSCLE: multiple sequence alignment with high accuracy and high throughput. *Nucleic Acids Res.* **32**, 1792–1797.

27. Gouy M, Guindon S, Gascuel O. 2010 SeaView Version 4: A Multiplatform Graphical User Interface for Sequence Alignment and Phylogenetic Tree Building. *Mol. Biol. Evol.* **27**, 221–224.

28. Guindon S, Dufayard J-F, Lefort V, Anisimova M, Hordijk W, Gascuel O. 2010 New algorithms and methods to estimate maximum-likelihood phylogenies: assessing the performance of PhyML 3.0. *Syst. Biol.* **59**, 307–321.

29. Darriba D, Taboada GL, Doallo R, Posada D. 2012 jModelTest 2: more models, new heuristics and parallel computing. *Nat. Methods* **9**, 772–772.

30. Guindon S, Gascuel O. 2003 A Simple, Fast, and Accurate Algorithm to Estimate Large Phylogenies by Maximum Likelihood. *Syst. Biol.* **52**, 696–704.

31. Kijas JW *et al.* 2012 Genome-Wide Analysis of the World's Sheep Breeds Reveals High Levels of Historic Mixture and Strong Recent Selection. *PLoS Biol.* **10**, e1001258.

32. Chaolong Wang Xiaowei Zhan Liming Liang Gonçalo R. Abecasis Xihong Lin. 2015 Improved Ancestry Estimation for both Genotyping and Sequencing Data using Projection Procrustes Analysis and Genotype Imputation. *Am. J. Hum. Genet.* **96**, 926–937.

33. Patterson N, Moorjani P, Luo Y, Mallick S, Rohland N, Zhan Y, Genschoreck T, Webster T, Reich D. 2012 Ancient admixture in human history. *Genetics* **192**, 1065–1093.

34. Pickrell JK, Pritchard JK. 2012 Inference of Population Splits and Mixtures from Genome-Wide Allele Frequency Data. *PLoS Genet.* **8**, e1002967.

35. Alexander DH, Lange K. 2011 Enhancements to the ADMIXTURE algorithm for individual ancestry estimation. *BMC Bioinformatics* **12**, 1–6.

36. Robinson JT, Thorvaldsdóttir H, Winckler W, Guttman M, Lander ES, Getz G, Mesirov JP. 2011 Integrative genomics viewer. *Nat. Biotechnol.* **29**, 24–26.

37. Miller W *et al.* 2012 Polar and brown bear genomes reveal ancient admixture and demographic footprints of past climate change. *Proc. Natl. Acad. Sci. U. S. A.* **109**, E2382–90.

38. Orlando L *et al.* 2013 Recalibrating Equus evolution using the genome sequence of an early Middle Pleistocene horse. *Nature* **499**, 74–78.

39. Librado P *et al.* 2015 Tracking the origins of Yakutian horses and the genetic basis for their fast adaptation to subarctic environments. *Proc. Natl. Acad. Sci. U. S. A.* **112**, E6889–97.

40. Sikora M *et al.* 2019 The population history of northeastern Siberia since the Pleistocene. *Nature* , 1.

41. Kistler L, Ware R, Smith O, Collins M, Allaby RG. 2017 A new model for ancient DNA decay based on paleogenomic meta-analysis. *Nucleic Acids Res.* **45**, 6310–6320.

42. Broushaki F *et al.* 2016 Early Neolithic genomes from the eastern Fertile Crescent. *Science* **353**, 499–503.

43. Allentoft ME *et al.* 2012 The half-life of DNA in bone: measuring decay kinetics in 158 dated fossils. *Proc. Biol. Sci.* **279**, 4724–4733.

44. Briggs AW, Stenzel U, Meyer M, Krause J, Kircher M, Pääbo S. 2010 Removal of deaminated cytosines and detection of in vivo methylation in ancient DNA. *Nucleic Acids Res.* **38**, e87.

45. Sawyer S, Krause J, Guschanski K, Savolainen V, Pääbo S. 2012 Temporal patterns of nucleotide misincorporations and DNA fragmentation in ancient DNA. *PLoS One* **7**, e34131.

46. Schwarz C, Debruyne R, Kuch M, McNally E, Schwarcz H, Aubrey AD, Bada J, Poinar H. 2009 New insights from old bones: DNA preservation and degradation in permafrost preserved mammoth remains. *Nucleic Acids Res.* **37**, 3215–3229.

47. Gilbert MTP *et al.* 2004 Ancient mitochondrial DNA from hair. *Curr. Biol.* **14**, R463–4.

48. Cassidy LM, Teasdale MD, Carolan S, Enright R, Werner R, Bradley DG, Finlay EK, Mattiangeli V. 2017 Capturing goats: documenting two hundred years of mitochondrial DNA diversity among goat populations from Britain and Ireland. *Biol. Lett.* **13**. (doi:10.1098/rsbl.2016.0876)

49. O'Sullivan NJ, Teasdale MD, Mattiangeli V, Maixner F, Pinhasi R, Bradley DG, Zink A. 2016 A whole mitochondria analysis of the Tyrolean Iceman's leather provides insights into the animal sources of Copper Age clothing. *Sci. Rep.* **6**, 31279.

50. Daly KG *et al.* 2018 Ancient goat genomes reveal mosaic domestication in the Fertile Crescent. *Science* **361**, 85–88.

51. Teasdale MD *et al.* 2017 The York Gospels: a 1000-year biological palimpsest. *R Soc Open Sci* **4**, 170988.

52. Metcalf JL *et al.* 2016 Microbial community assembly and metabolic function during mammalian corpse decomposition. *Science* **351**, 158–162.

53. Pereira F, Davis SJM, Pereira L, McEvoy B, Bradley DG, Amorim A. 2006 Genetic signatures of a Mediterranean influence in Iberian Peninsula sheep husbandry. *Mol. Biol. Evol.* **23**, 1420–1426.

54. Chen S-Y, Duan Z-Y, Sha T, Xiangyu J, Wu S-F, Zhang Y-P. 2006 Origin, genetic diversity, and population structure of Chinese domestic sheep. *Gene* **376**, 216–223.

55. Demirci S, Baştanlar EK, Dağtaş ND, Pişkin E, Engin A, Özer F, Yüncü E, Doğan ŞA, Togan İ. 2013 Mitochondrial DNA Diversity of Modern, Ancient and Wild Sheep (Ovis gmelinii anatolica) from Turkey: New Insights on the Evolutionary History of Sheep. *PLoS ONE*. **8**, e81952. (doi:10.1371/journal.pone.0081952)

56. Rast-Eicher A. 2016 *Fibres: Microscopy of Archaeological Textiles and Furs*. Budapest: Archaeolingua Alapítvány.

57. Rast-Eicher A. 2010 Fell- und Lederreste aus den Gräbern 2008. In *Spiez-Einigen, Holleeweg 3, Naturwissenschaftliche Untersuchungen zu den bronzezeitlichen Bestattungen* (eds C Cooper, M Harbeck, M Kühn, A Rast-Eicher, M Schweissing, S Ulrich-Bochsler, P Vandorpe), pp. 175–198. Bern: Service Archéologique du Canton de Berne.